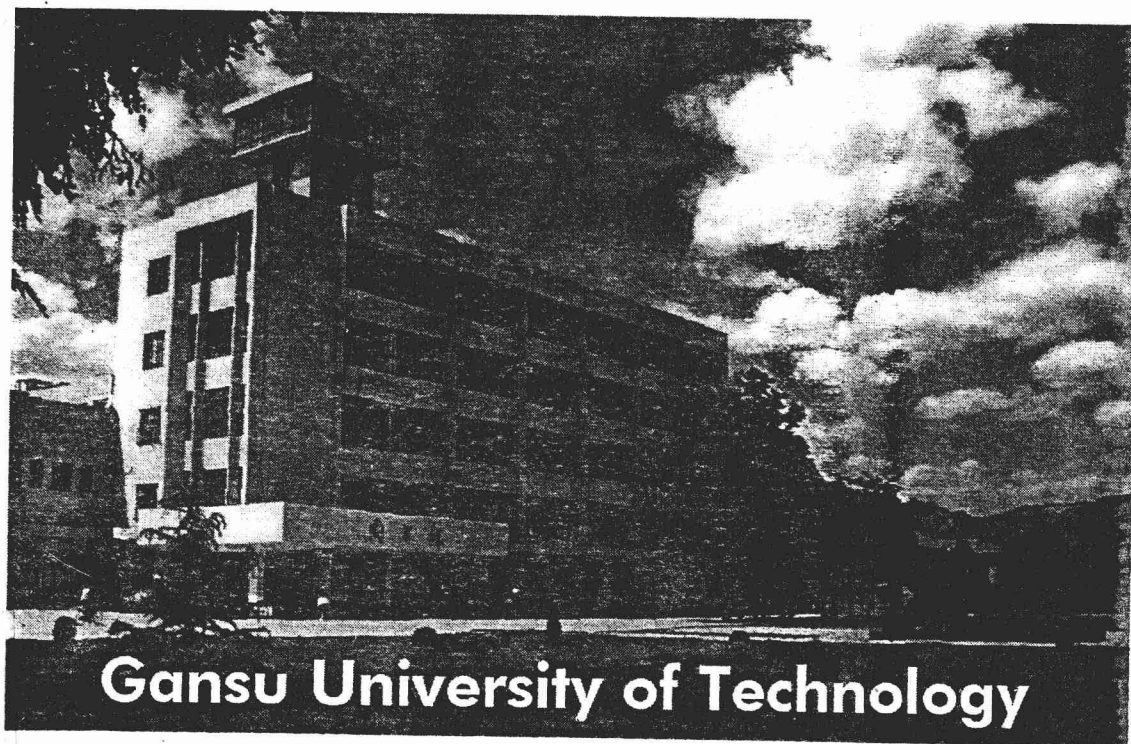


甘肃工业大学材料加工工程学科

陈剑虹教授论文选集



一九九七年七月

陈剑虹教授简介

陈剑虹，男，生于1937年5月13日，清华大学焊接专业研究生毕业，现甘肃工业大学焊接专业教授，国家级有突出贡献的科技专家，中国机械工程学会焊接学会副理事长，甘肃工业大学前任校长。

陈剑虹教授几十年来一直从事焊接及金属材料学科的科学研究。在焊接电弧物理及焊接化学冶金有系列理论研究成果，在此基础上研制的焊条、电弧分析仪、计算机辅助焊接工艺选择系统分别获全国科学大会奖、国家“七五”攻关重大成果奖及省部二、三等奖，共取得二项发明专利。在HSLA钢低温解理断裂机理方面取得重要研究成果，提出同一种钢在不同缺陷尖锐度的试件上解理断裂的临界事件是可变的；对该领域主要物理模型(RKR)提出了修正，修改了解理断裂判断准则，并提出统计模型；提出微观断裂应力是一个比目前广泛采用的宏观断裂韧性参数更稳定的参数，可用作评定韧性的工程参量，上述有关论点的系列论文(共计19篇)发表于金属权威杂志(Metal. Trans., Acta Metall. 和 Inter. J. Fract.)，1995年就上述专题在美国哈佛大学和依阿华州立大学进行讲学，受到国内外学者的好评。

近年来共发表论文60余篇，其中发表于国际著名杂志28篇，于国际会议宣读5篇(以邀请报告宣读)。国际杂志发表的论文均被SCI和EI收录。1994年主持“新型材料焊接连接涂敷及表面改质国际讨论会”(47届国际焊接年会会前会)，并主编了英文论文集。

1985-1995年担任甘肃工业大学校长期间，以学科建设为主要工作，学校硕士点由2个增至9个，学校学术水平有明显提高，教学改革有重要进展。

目 录

断裂机理的研究

1. **Advances in the mechanism of cleavage fracture of low alloy steel at low temperature. Part I: Critical event**, Int. J. Fract. Vol. 83 No.2, p105~120, 1997 1
2. **Advances in the mechanism of cleavage fracture of low alloy steel at low temperature. Part II: Fracture model**, Int. J Fract. Vol. 83 No.2, p121~138, 1997 19
3. **Advances in the mechanism of cleavage fracture of low alloy steel at low temperature. Part : III Local fracture stress σ_f** , Int. J Fract. Vol. 83 No.2, p139~157, 1997 37
4. **A Statistical Model for Cleavage Fracture of Low Alloy Steel**, Acta Mater. Vol. 44, p3979~3989, 1996 56
5. **The Local Fracture Stress σ_f as a Fracture Toughness Parameter Characterize an Heterogeneous weld zone**, Fatigue & Fract. of Engng Mater. & Struct. Vol. 19, p807~819, 1996 67
6. **A Comparison of Fracture Behavior of Low Alloy Steels with Different Sizes of Carbide Particles**, Metall. & Mater. Trans. Vol. 27A, p1909~1917, 1996 81
7. **Micromechanism of the transition of fibrous cracking to cleavage of C-Mn base and weld steel**, Metall. and Mater. Trans. Vol. 25A, p1381~1390, 1994 93
8. **Further study on the mechanism of cleavage fracture at low temperature**, Acta Metall. & Mater. Vol. 42, p251~261, 1994 106
9. **Critical assessment of local Cleavage stress σ_f in Notch Specimens of C-Mn steel**, Metall. and Mater. Trans. Vol. 24A, p1381~1389, 1993 117
10. **Further investigation of the critical events in cleavage fracture σ_f C-Mn base and weld steel**, Metall. and Mater. Trans. Vol. 24A, p659~667, 1993 129
11. **Study on the impact toughness of the C-Mn Multi-layer weld metal at -60°C**, Welding Journal Vol. 72, p19s ~27s, 1993 141

12. A Comparison of toughness of C-Mn steel with different grain sizes, Metall. Trans. Vol. 23A, p2549~2556, 1992	152
13. Study of Mechanism of Cleavage Fracture at Low Temperature , Metall. Trans. Vol. 23A, p509~517, 1992	163
14. Further study on the scattering of the local fracture stress and allied toughness values, Metall. Trans. Vol. 22A ,p2287~2296, 1991	172
15. On the scattering of the local fracture stress σ_f , Acta Metall. & Mater. , Vol. 38, p2527~2535, 1990	185
16. Fracture behavior of C-Mn steel and weld metal in notched and precracked specimens : Part I . Fracture behavior , Metall. Trans. Vol. 21A, p313~320, 1990	194
17. Fracture behavior of C-Mn steel and weld metal in notched and precracked specimens : Part II. Micromechanism of fracture , Metall. Trans. Vol. 21A, p321~330, 1990	205
18. Fracture behavior of C- Mn steel multipass MMA weld metals at -60°C in Charpy V testing , Materials Science and Technology Vol. 4, p732~739, 1988	215
19. Micro-fracture behavior induced by M-A Constituent (Island Martensite) in simulated welding heat affected zone of HT80 high strength low alloying steel, Acta Metall. & Metall. Vol. 32, p1779~1788, 1984	224
20. 高強力鋼溶接部の破壊発生伝播に及ぼす島状マルテンサイトの影響, 材料 Vol.34,p18~22,1985	235

焊接电弧物理与化学冶金

21. Study on the mechanism of spatter produced by basic welding electrodes, Welding Journal Vol. 75, p311s ~ 316s, 1996	240
22. The transfer of small amount of boron during SMA welding, Welding Journal Vol. 70 , p277s~285s, 1991	248
23. Investigation of the kinetic process of metal-oxygen reaction during shielded metal arc welding ,	

Welding Journal Vol. 68, p245s~251s, 1989	259
24. A Study of the mechanism for globular metal transfer from covered electrodes , Welding Journal Vol. 68, p145s~150s, 1989	268
25. 手工电弧焊过程微量硼过渡及其稳定性研究, 焊接学报 Vol. 10, No. 3, p139~146, 1989	276
26. 手工电弧焊氧化还原反应动态过程的研究, 焊接学报 Vol. 9, No. 2, p59~68, 1988	284
27. 焊条电弧力的测定研究, 焊接学报 Vol. 8, No. 3, p107~112, 1987	294
28. HT80高强钢模拟焊接HAZ透射电镜组织观察及位错密度测定, 焊接学报 Vol. 6, No. 4, p157~162, 1985	300
29. 碱性焊条发尘致毒影响因素的研究, 焊接学报 Vol. 1, No. 2, p53~65, 1980	308

陶瓷连接

30. The Metallurgical behaviour during brazing of Ni-base alloy Inconel 600 to Si₃N₄ with Ag₇₁Cu₂₇Ti₂ filler metal J. Materials Science Vol. 28, p2933~2942, 1993	323
31. Segregation of chromium at the interface between Ni-Cr-Si-Ti brazing filler metal and Si₃N₄ Ceramics J. Materials Science Letter Vol. 12A, p87~89, 1993	334
32. An observation of the overflow of Ag-Cu-Ti filler metal on the surface of Ni-base Alloy Inconel 600, J. Materials Science Letter Vol. 11A, p1473~1475, 1992	338

专 著 (简介及目录)

33. 《焊接卫生与安全》 机械工业出版社, 北京, 1987年	342
34. 《焊接材料及其冶金》 机械工程师进修大学, 北京, 1989年	359
35. “Welding Joining Coating and Surface Modification Of Advanced Materials” , Proceeding of the Pre-Assembly symposium of 47th Annual Assembly of IIW, 1-2 Sep 1994, Dalian, China (Vol. I & Vol. II)	364

注:

- | | |
|--|-------------------|
| 1. Int. J Fract. | 《美国国际断裂杂志》 |
| 2. Acta Metall. & Mater. | 《美国材料冶金学报》 |
| 3. Fatigue & Fract. Engng Mater. & Struct. | 《英国工程材料和结构的疲劳和断裂》 |
| 4. Metall. and Mater. Trans. | 《美国冶金与材料汇刊》 |
| 5. Welding Journal | 《美国焊接杂志》 |
| 6. J. Materials Science | 《材料科学杂志》 |
| 7. J. Materials Science Letter | 《材料科学杂志》(通讯) |

international journal of fracture

PUBLISHED TWICE MONTHLY

TABLE OF CONTENTS

Advances in the mechanism of cleavage fracture of low alloy steel at low temperature. Part II: Critical event

JH CHEN, G.Z. WANG,
C. YAN, H. MA and J. ZHANG

Advances in the mechanism of cleavage fracture of low alloy steel at low temperature. Part II: Fracture model

JH CHEN, G.Z. WANG,
C. YAN, H. MA and J. ZHANG

Advances in the mechanism of cleavage fracture of low alloy steel at low temperature. Part III: Local fracture stress σ_f

JH CHEN, G.Z. WANG,
C. YAN, H. MA and J. ZHANG

Analysis of crack growth rate based on rotation at the crack tip plastic zone

A. BHATTACHARYA

A proposed method for the applicability of load separation condition in pre-cracked specimens

A.M. CASSAROVICH and
E.A. DE VRIES

On phase transition layers in certain micro-damaged two-phase solids

E. DEBIESSON and
G.Z. WOZNIAK

Crack growth criteria incorporating non-singular stress: Size effect in apparent fracture toughness

A.W. DYSKIN

Editor: SCHERRER, Editor-in-Chief:
The Committee of Royal Academy



EZ0001031

kluwer academic publishers

international journal of
fracture

Vol. 83, No. 2, 1997

TABLE OF CONTENTS

<u>Advances in the mechanism of cleavage fracture of low alloy steel at low temperature. Part I: Critical event</u>	<u>J.H. CHEN</u> , G.Z. WANG, C. YAN, H. MA and L. ZHU	105-120
<u>Advances in the mechanism of cleavage fracture of low alloy steel at low temperature. Part II: Fracture model</u>	<u>J.H. CHEN</u> , G.Z. WANG, C. YAN, H. MA and L. ZHU	121-138
<u>Advances in the mechanism of cleavage fracture of low alloy steel at low temperature. Part III: Local fracture stress σ_f</u>	<u>J.H. CHEN</u> , G.Z. WANG, C. YAN, H. MA and L. ZHU	139-157
Analysis of crack growth rate based on rotation at the crack tip plastic zone	A. BHATTACHARYA	159-165
A proposed method for the applicability of load separation condition in precracked specimens	A.N. CASSANELLI and L.A. DE VEDIA	167-173
On phase transition layers in certain micro-damaged two-phase solids	F. DELL'ISOLA and CZ. WOŹNIAK	175-189
Crack growth criteria incorporating non-singular stresses: Size effect in apparent fracture toughness	A.V. DYSKIN	191-206

Letters in fracture and micromechanics (blue pages)

Meetings calendar		L16
Dislocation thermal activation analysis of temperature and strain rate dependence of fracture toughness in structural steels	WEI-SHENG LEI and YAN SU	L17-L23
Stress intensity factors for the penny-shaped crack problem under concentrated force loading	Y.Z. CHEN and Z.J. PENG	L25-L29

Advances in the mechanism of cleavage fracture of low alloy steel at low temperature. Part I: Critical event

J.H. CHEN, G.Z. WANG, C. YAN, H. MA and L. ZHU

Gansu University of Technology, Lanzhou, Gansu, People's Republic of China, 730050

Received 20 April 1995; accepted in revised form 28 June 1996

Abstract. The critical event of cleavage is variable for different types of specimens made of the same steel. In notched specimens (Charpy V or 4 PB) over a wide temperature range as low as -196°C , the critical event is the propagation of a ferrite grain-sized crack ($30\text{--}40\text{ }\mu\text{m}$). In precracked specimens at a moderately low temperature (around -110°C) it is the propagation of a second phase particle-sized crack ($< 10\text{ }\mu\text{m}$). At ever lower temperatures (-150°C – -196°C) the cleavage fracture is nucleation-controlled.

No matter whether a notched specimen or a precracked specimen is used, as long as a fibrous crack has been initiated and propagated in it, the critical event is the propagation of a ferrite grain-sized crack and the fracture behavior can be handled as in a specimen with an acute notch.

The difference of ' σ_f ' values measured in a notched specimen and a precracked specimen is caused by a change of the critical event in these two specimens.

1. Introduction

Discussing the critical event of cleavage fracture Smith clarified 'In developing a realistic physical model of the cleavage process it is of paramount importance to ascertain the nature of the critical event in the formation of a cleavage crack. ... It is essential to decide if the greatest difficulty in the formation of a crack is its nucleation or whether it occurs at some stage during its growth' [1].

Before the early 50s', crack nucleation was considered to be the most difficult step, i.e. the critical event during the fracture process. This was based on the Stroh model [2] which suggested that the crack could be nucleated by a dislocation pile-up at an energy balance higher than that needed for crack propagation. Yet a number of experiments confirmed the important influence of the hydrostatic tension and tensile stress on the cleavage fracture, [3, 4], which implied that the controlling step was crack propagation rather than crack initiation. Observations of grain-sized micro-cracks remaining in fracture specimens [5] supported this argument and exemplified grain boundary control. On the basis of the dislocation pile-up model and the above observation of the remaining ferrite grain-sized crack, in the late 50s' and early 60s' crack propagation was identified as the critical event and the grain size was identified as the dominant microstructure feature for cleavage fracture [6–7]. Relationships between toughness parameters such as the brittle-tough transition temperature T_c , the local fracture stress σ_f and the grain sizes were observed.

Yet this model could not explain the influence of second phase particles on the variation of toughness for similar grain sizes and yielding stress, which was observed by McMahon and Cohen [8]. They also observed that the majority of the ferrite micro-cracks originated at carbide cracks. Smith [9] proposed a well-known model: a grain boundary carbide particle was cracked by an impinging dislocation pile-up and the microscopic carbide crack acted as a Griffiths crack. The critical event is the propagation of the carbide crack into the neighboring

ferrite grain as a result of the combined action of the dislocation pile-up and the applied normal stress. The fracture stress could be calculated by the following equation.

$$\left(\frac{Co}{d}\right) \sigma_f^2 + \tau_e^2 \left\{ 1 + \frac{4}{\pi} \left(\frac{Co}{d}\right)^{1/2} \frac{\tau_i}{\tau_e} \right\}^2 \geq \frac{4E\gamma p}{\pi(1-\nu^2)d}, \quad (1)$$

where Co is the thickness of a grain boundary carbide, d is the grain diameter, τ_e is the effective shear stress, τ_i is the lattice friction stress, and γp is the effective surface energy of ferrite.

This model supplied a mechanism for an increase in effective surface energy subsequent to crack initiation which supported the model of propagation control.

Curry and Knott [10] modified this model further by rewriting the τ_e as $kd^{-1/2}$ and reducing (1) to

$$\sigma_f^2 + \frac{k^2}{Co} \left\{ 1 + \frac{4}{\pi} (Co)^{1/2} \frac{\tau_i}{k} \right\}^2 \geq \frac{4E\gamma p}{\pi(1-\nu^2)Co} \quad (2)$$

k is the shear Hall-Petch yielding constant. In this equation the only microstructural parameter affecting the fracture stress is the carbide thickness. The authors concluded that the cleavage strength depends on the carbide thickness rather than the grain size. They attributed the strong dependence of σ_f on the grain sizes to the relationship between ferrite grain sizes and the largest observed carbide thicknesses in normalized and annealed mild steel.

Thus from the late 60s' to the 80s' the critical event of cleavage was held as the propagation of a second phase particle micro-crack into the matrix. The particle sizes are clearly the most important dimensions.

Hahn [11] summarized the work of the past two decades as saying 'The implications of crack blunting are related to the essential role of carbide particle and other brittle phases in the steel. Dislocation pile-ups and ferrite grain size are accorded a diminished role'.

Based on the RKR model [12] and taking the 'eligible carbide crack' as the events, a number of statistical models were established [13-15].

But during this period some researchers proposed that the critical event of cleavage could be changed from one type to another type of specimen made of the same material or from one temperature to another [16, 17].

Oates and Griffiths claimed that 'In the tensile tests of 3 percent silicon iron, the critical event for fracture throughout -196 to -50°C was the nucleation of a suitable microcrack. Between -50°C and $+50^\circ\text{C}$ the critical event was the growth of grain-size microcracks themselves nucleated at cracks in grain-boundary carbides or pearlite colonies. The deformation and fracture mechanisms in the notched specimens were in sharp contrast to those described above. Throughout the range -160°C to $+40$ twins were not formed at the fracture stress and fracture was determined by the growth of slip-nucleated carbide cracks'. The authors attribute the change in the critical event from the growth of ferrite microcracks (found in smooth specimens) to the growth of carbide cracks (found in notched specimens) to the difference of high strained volume in these two types of specimens. Lin, Evans, and Ritchie [17] proposed that 'At the lowest temperature cleavage fracture occurs once the nucleation condition is satisfied. Nucleation dominated behavior would then pertain. At higher temperatures particles which satisfy the dynamic criterion for propagation across the particle/matrix interface would then become the source of cleavage fracture. At still higher temperatures, the particle may crack

Table 1. Composition of C-Mn steel and weld steels, wt%.

Materials	C	Mn	Si	S	P	Ti	B	O	N	Ni
C-Mn base metal	0.18	1.49	0.36	0.033	0.01	*	*	*	*	*
C-Mn weld metals	0.07	1.24	0.28	0.02	0.01	0.03	*	0.03	0.019	*
Ti-B weld metals	0.06	1.49	0.48	0.02	0.01	0.03	0.004	0.03	0.019	*
Ti-B-Ni weld metals	0.07	1.60	0.19	0.031	0.02	0.02	0.003	0.03	0.019	0.45

* Not measured.

and the crack can extend to the first grain boundary without causing failure, stable grain size cracks would then become possible. Within this temperature range, cleavage fracture would occur when a crack can extend dynamically across the ferrite grain boundary'. The authors attributed the change in the critical event from crack nucleation (at the lowest temperature) to the carbide crack growth (at higher temperatures) and then to the ferrite grain crack growth (at still higher temperatures) to the variation of relative values among the yield stress, carbide cleavage strength and ferrite grain strength at various temperatures.

Another important parameter associated with the critical event is the local fracture stress σ_f . A change of σ_f values measured in notched and precracked specimens is observed, but just like the variation of the critical event, it is attributed to the different high stress volumes in these two specimens [11].

On the basis of the work [18–25] done by authors on the critical event, the present paper provides a comprehensive discussion especially on the renovating concepts of the critical event, its variability and its effect on the local fracture stress σ_f .

2. Experimental procedure

2.1. MATERIALS

The materials used were C-Mn steel and C-Mn, Ti-B, and Ti-B-Ni weld steels with composition shown in Table 1.

2.2. SPECIMENS

The standard Charpy V specimens with root radius $\rho = 0.25$ mm were used. Three types of deep notched specimens for 4 point bending (4PB) test, i.e. single notch ($\rho = 0.25$ mm, Griffiths–Owen specimen), double notches ($\rho = 0.25$ mm) and single notch with different root radii ($\rho = 0.05, 0.075, 0.15, 0.25, 0.35, 0.6, 1.0$ mm) were adopted. Precracked specimens for the three point bending test (COD) were used also. Dimensions of specimens are shown in Figure 1.

2.3. EXPERIMENTAL METHOD

2.3.1. Toughness testing procedure

For investigation of the critical event of cleavage fracture occurring in the lower shelf temperature region the Charpy V impact tests were carried out at -45°C and -60°C at a hammer speed of 5 m/sec. Most of the 4PB tests were carried out at -196°C and a part at -150°C , the latter having a root radius of 0.25 mm. COD tests were carried out at -70°C , -90°C ,

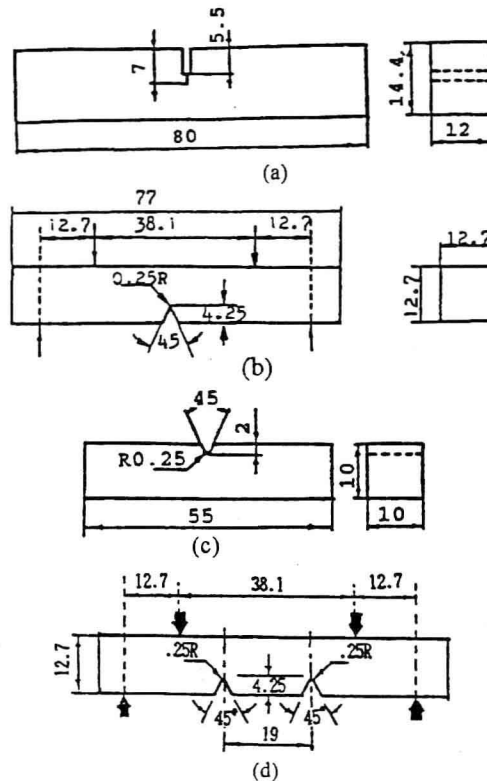


Figure 1. Dimensions of toughness specimens: (a) COD, (b) 4 PB, (c) Charpy V and (d) double notches.

-110°C and -196°C and some of the COD specimens were unloaded at 95 percent of fracture load. For investigation of the critical event of cleavage fracture occurring at the transition temperature after a fibrous crack had been initiated and propagated, the COD test was carried out within a range of -80°C to $+15^{\circ}\text{C}$, the 4 PB test -90°C to -10°C , the Charpy V test at -20°C and -40°C . The cross-head speed of the testing machine in both 4 PB and COD tests was 1 mm/min. The routine properties σ_y and n were measured by tensile tests at various temperatures.

2.3.2. Determining the critical event

Several metallographic sections as shown in Figure 2(a) were taken from 4 PB, COD and Charpy V specimens to observe the remaining microcracks which were initiated but were shorter than the critical length for unstable propagation and remained in the specimens. The remaining crack below the survived notch in the fractured double-notched 4 PB specimens and in the COD specimens unloaded prior to fracture were observed especially carefully. The microstructural feature limiting the maximum length of the remaining crack was defined as the microstructural domain of the critical event.

The sizes of the ferrite grains in the zone where the cleavage crack was initiated were measured in a special metallographic section, shown in Figure 2(b). The relationships between these grain sizes or the maximum lengths of remaining cracks and macro-mechanical properties were used to determine the critical event. The fracture surfaces were observed in detail

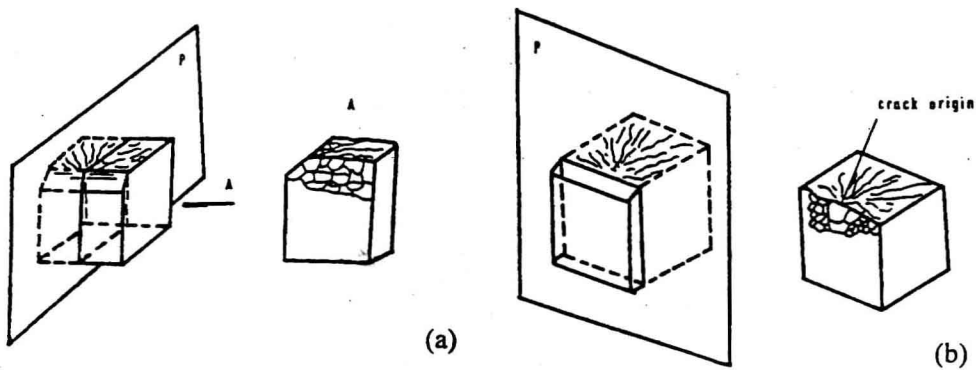


Figure 2. Metallographic sections for examining: (a) the remaining cracks and (b) microstructure of region where cleavage cracks were initiated.

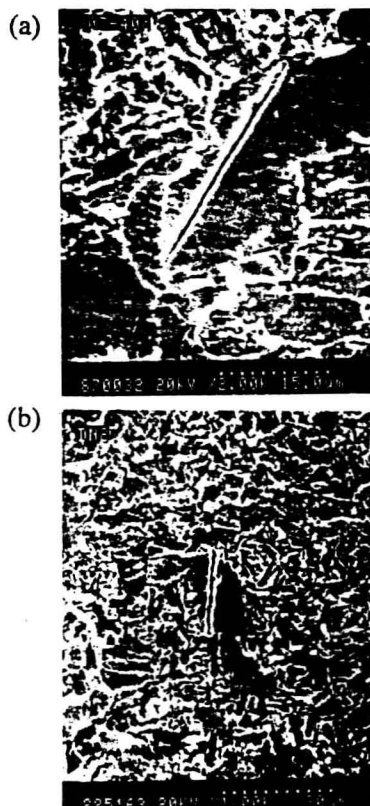


Figure 3. Ferrite grain-sized cracks remaining in: (a) Charpy V specimen at -40°C and (b) double notched 4 PB specimen at -150°C .

using a scanning electron microscope (SEM) and the sizes of second phase particles initiating the cleavage crack and the sizes of the cleavage facets around them were measured to give additional information for determining the critical event.



Figure 4. Ferrite grain-sized cracks remaining in 4PB specimens with notch root radius: (a) $\rho = 0.075$ mm, $L = 10 \mu\text{m}$, (b) $\rho = 0.25$ mm, $L = 25 \mu\text{m}$ and (c) $\rho = 0.6$ mm, $L = 25 \mu\text{m}$ at -196°C , where L represents the length of remaining crack.

2.3.3. Calculating the local cleavage fracture stress ' σ_f '

The σ_f has been evaluated accurately from the Charpy V, 4PB and COD testing. The detailed methods are described in Part III of the present paper [26].



Figure 5. Second phase particle-sized remaining crack in COD specimen under -110°C .

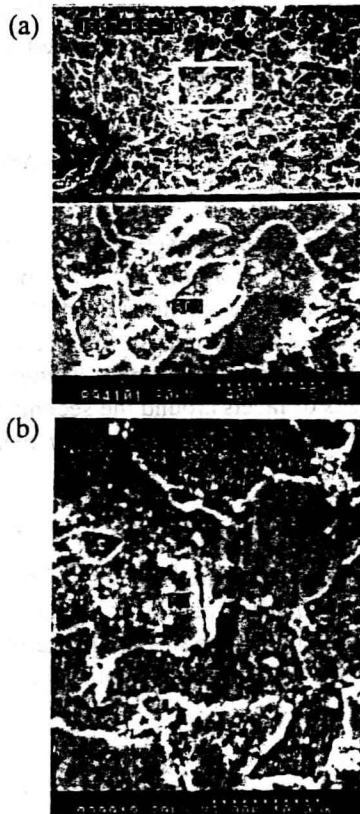


Figure 6. Remaining crack observed in COD specimen unloaded at -70°C : (a) crack tip opening $< 40\ \mu\text{m}$, $L = 5.5\ \mu\text{m}$ and (b) crack tip opening of $65\ \mu\text{m}$, $L = 17\ \mu\text{m}$, L : crack length.

3. Experimental results

3.1. CRITICAL EVENT OBSERVED IN SPECIMENS

The remaining ferrite grain-sized cracks were found in fractured Charpy V specimens at -40°C and -60°C , as shown in Figure 3(a) and similar cracks were observed below the tips of survived notches in the double notched 4 PB specimens at -150°C also (Figure 3(b)).

Further, as shown in Figure 4 the ferrite grain-sized cracks were observed in fractured 4 PB specimens with different notch root radii tested at -196°C .

In COD specimens unloaded at 95 percent of fracture load at -110°C , only the remaining second phase particle-sized cracks were observed, as shown in Figure 5. In COD specimens unloaded at 95 percent of fracture load at -70°C , as the crack tip opening was narrow ($< 40\text{ }\mu\text{m}$), only the second phase particle-sized cracks were observed (Figure 6(a)). However ferrite grain-sized cracks could be found when the tip opening was wider ($65\text{ }\mu\text{m}$, Figure 6(b)).

It was observed that no matter whether a notched or a precracked specimen was used, once a fibrous crack was initiated and propagated in it, the remaining ferrite grain-sized cracks could be found at distances from the fibrous crack tip in unloaded specimens, as shown in Figure 7.

In COD specimens unloaded at -196°C , the original tip width $b = 0.23\text{ }\mu\text{m}$ of the fatigue precrack was blunted to $b = 1.5\text{ }\mu\text{m}$. None of the remaining microcracks could be found.

The statistical distribution of remaining crack lengths in Charpy V specimens at -45°C and -60°C and COD specimens at -110°C are indicated in Figure 8. An apparent difference of the maximum length of remaining cracks found in notched specimens ($30 \sim 40\text{ }\mu\text{m}$) and in precracked specimens ($< 10\text{ }\mu\text{m}$) is indicated.

3.2. RELATIONSHIP BETWEEN THE MECHANICAL PROPERTIES AND MICROSTRUCTURAL PARAMETERS

As shown in Figure 9(a) and 9(b), in Charpy V specimens, there are apparent relationships between the Charpy V absorbed energy and both the sizes of ferrite grains in the region of cleavage initiation (Figure 9(a)) and the maximum lengths of remaining ferrite cracks (Figure 9(b)). Yet as shown by Figure 10 the relation between the toughness and the sizes of second phase particles initiating cleavage is highly scattered and therefore less clear. Additionally, in Figure 11, the sizes of facets around the second phase particles initiating the cleavage crack were related to the cleavage fracture stress σ_f measured in 4 PB specimens.

3.3. RESULTS OF MEASUREMENT

The cleavage fracture stress values σ_f measured in notched and precracked specimens are shown in Table 2. A jump of 600–800 MPa from the values of notched specimens to that of precracked specimens was observed for all three steels. The statistical distribution of the sizes of second-phase particles which initiated the cleavage cracks are plotted in Figure 12(a) and 12(b).

4. Discussion

4.1. CRITICAL EVENTS FOR VARIOUS SPECIMENS AT DIFFERENT TEMPERATURES

From Figure 3 it is clearly shown that for notched specimens tested by either dynamic loads (at -60°C) or static loads (at -110°C to -196°C) the boundary between ferrite grains is the last barrier for the propagation of a crack that has just been nucleated. Therefore in notched specimens the critical event for cleavage fracture was identified as the propagation of a ferrite grain-sized crack to neighboring grains.

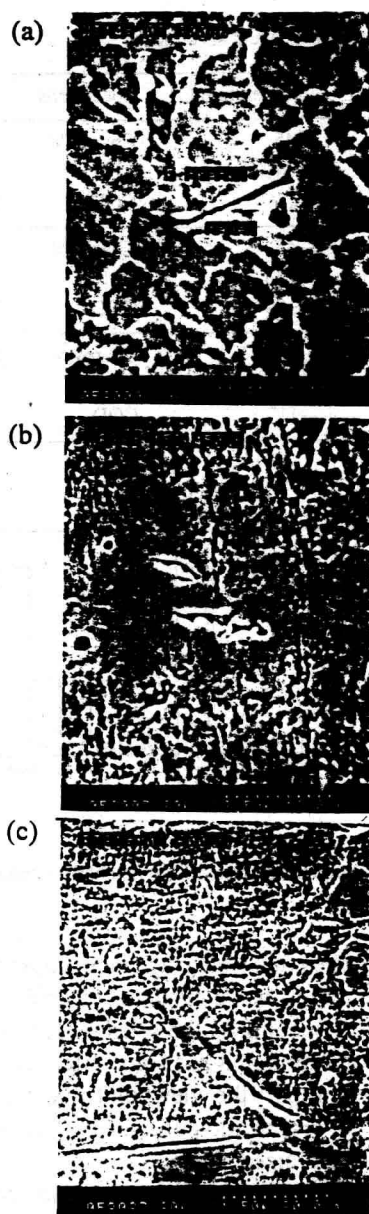


Figure 7. Ferrite grain-sized cracks at distances from the tips of fibrous cracks observed in both COD precracked and 4 PB notched specimens unloaded prior to fracture: (a) weld metal COD specimen, (b) base metal COD specimen and (c) weld metal 4 PB specimen.

Figure 9 shows a sharp rise of toughness when the ferrite grain size or the maximum length of the remaining crack is less than $40\text{ }\mu\text{m}$. This indicates that the critical length for cleavage crack propagation in Charpy V specimens is around $40\text{ }\mu\text{m}$.

In the 4 PB test, when the size of the cleavage facet was less than $40\text{ }\mu\text{m}$, it was found to have a definite relation with σ_f (Figure 11) and this could be considered as further evidence of grain-sized crack critical event. On the other hand, when the facet is more than $40\text{ }\mu\text{m}$, σ_f